https://doi.org/10.14669/AM.VOL95.ART4

NONLINEAR METHOD OF PRECRASH VEHICLE VELOCITY DETERMINATION BASED ON TENSOR PRODUCT OF LEGENDRE POLYNOMIALS – LUXURY CLASS

ŁUKASZ GOSŁAWSKI[1], EWA SYS[2], ADAM MROWICKI[3], MATEUSZ KRUKOWSKI[4], YANLIN MA[5], PRZEMYSLAW KUBIAK[6]

Abstract

Presented paper discusses a new, nonlinear approach to EES (Equivalent Energy Speed) parameter determination in frontal car collisions. This method is based on tensor product of Legendre polynomials and in this case considers Luxury car class. Methods that are used up till now are based on a linear dependency between mass, velocity and deformation. This is of course a simplification that was necessary, due to limitation in computation power of computers when this method was introduced decades ago. The contemporary resources allowed Authors to develop a much more sophisticated method. The mathematical model was developed using data shared by National Highway Traffic Safety Administration (NHTSA). This database covers a large number of test cases along with various information including vehicle mass, crash velocity, chassis deformation etc. New method proves to be more accurate than the currently used approach utilizing linear dependency of deformation force and deformation of the vehicle.

Keywords: Car Crash Reconstruction; Car Accidents; Tensor Product System; Inverse System; EES

1 Institute of Vehicles and Construction Machinery Engineering, Warsaw University of Technology, Ludwika Narbutta 84, 02-524 Warsaw, Poland, e-mail: lukasz.goslawski.dokt@pw.edu.pl, ORCID: 0000-0002-3369-5510

2 Institute of Vehicles and Construction Machinery Engineering, Warsaw University of Technology, Ludwika Narbutta 84, 02-524 Warsaw, Poland, e-mail: ewa.sys.dokt@pw.edu.pl, ORCID: 0000-0001-5568-7039

3 Institute of Vehicles and Construction Machinery Engineering Warsaw University of Technology, Ludwika Narbutta 84, 02-524 Warsaw, Poland, e-mail: adam.mrowicki.dokt@pw.edu.pl, ORCID: 0000-0002-7865-099X

4 Institute of Mathematics, Łódź University of Technology, Żeromskiego 116, 90-924, Łódź, Poland, e-mail: mateusz.krukowski@p.lodz.pl, ORCID: 0000-0001-6644-5633

5 School of Transportation Science and Engineering, Harbin Institute of Technology, 73 Huanghe Road, Nangang District, Harbin 150090, China, e-mail: mayanli@hit.edu.cn, ORCID: https://orcid.org/0000-0003-1476-424X

6 Institute of Vehicles and Construction Machinery Engineering, Warsaw University of Technology, Ludwika Narbutta 84, 02-524 Warsaw, Poland, e-mail: przemyslaw.kubiak@pw.edu.pl, ORCID: 0000-0003-0225-9609 Institute of Marketing and Sustainable Development, Lodz University of Technology, Piotrkowska 266, 90-924 Łódź, Poland

https://doi.org/10.14669/AM.VOL95.ART4

1. Introduction

One of the most basic sources of information for crash site investigators is the scene reconstruction [3, 6, 34]. It is based on evidence or marks that appear as a result of a collision. Such marks, if properly analyzed and processed are invaluable to determine the course of the crash and its immediate cause [2, 18, 23]. The scope of reconstruction depends mainly on the amount and quality of the evidence [11, 32, 35]. Unfortunately, in everyday practice is it uncommon that a set of evidence gathered at the scene of investigation is sufficient to fully recreate the course of the crash. Depending on the data, reconstruction may only describe certain events or its fragments. Therefore, investigators quite frequently utilize advanced software tools that enable them to determine certain quantities, that cannot be easily determined from the obtained data.

The procedure that investigators use to reconstruct the scene is based on calculation of varying degree of complexity, mainly due to the mathematical model utilized to describe the events. Such models, however, do not describe the events in a perfectly accurate manner, as it is impossible to include all factors and events that took place.

Currently, the most popular method used for precrash velocity determination based on car deformation is CRASH3 [19, 20, 22]. This approach uses two algorithms. The first one calculates the vehicle trajectory, using the law of energy conservation [30, 31, 38], also taking into account the rotational motion of the vehicle [24, 25, 36]. The second algorithm is analyzing deformation of the vehicle, that extrapolates and interpolated the already available data. This approach is based on the most popular, linear model of velocity and deformation dependency. This method was introduced in 1980s and as the standard of vehicle construction changed over time (monocoque chassis, use of composite materials and plastics, use of High Strength Steels and other advanced materials [5]), the error in precrash velocity determination has been also rising. Also considering the advancements in computation power of contemporary computers, that are unparallel in terms of amount of processed data and the time they need to accomplish the task, as compared to the units when this method was initially introduced. Nevertheless, this method is still widely used, despite being outdated, since there is no viable alternative for it.

Considering the above-mentioned situation, Authors decided to introduce a nonlinear method that is more accurate and that would fully utilize the computing power nowadays and take into consideration the advancements in automotive industry.

In the linear approach the deformation force is a function of vehicle deformation and the stiffness coefficient b_k is the slope of this function. In other words, the linear method assumes the b_k coefficient to be constant, whereas the main assumptions of nonlinear method are:

- b_k coefficient is nonlinearly dependent on deformation C_S and mass m,
- b_k coefficient is nonlinearly dependent on dent zone width,
- one can divide all the cases into classes based on vehicle mass [15, 28, 37].

https://doi.org/10.14669/AM.VOL95.ART4

To determine the EES (Equivalent Energy Speed) the following equation (1) is used:

$$EES = \sqrt{\frac{2W_{\mathrm{def}}}{m}} \tag{1}$$

The EES parameter represents the energy, that is used on deformation of the vehicle while impacting a rigid obstacle [26, 29, 33]. During impact, if the velocity exceeds 11.5 $\frac{\mathrm{km}}{\mathrm{h}}$ then only plastic deformations occur, and the entire kinetic energy accumulated by the vehicle is transferred to deformation work. The pre-crash velocity $\mathrm{V_t}$ is a function of stiffness coefficient b_k and deformation coefficient C_s [12, 16, 21]. This coefficient is obtained as a weighted average of deformation depth measured in six control points C_1 "to" C_6 [9, 10, 14], according to the following formula (2):

$$C_s = \frac{(\frac{C_1}{2} + \mathrm{C2} + \mathrm{C3} + \mathrm{C4} + \mathrm{C5} + \frac{C_6}{2})}{5} \tag{2}$$

In this approach Authors created a nonlinear model describing the Luxury vehicle class, using Legendre polynomials and inverse systems [1, 4] which will be elaborated in the following section.

The model was based on a database provided by NHTSA. This organization is enforcing vehicle performance standards and is working with local and state governments to increase the safety on the roads, reduce casualties [17], injuries and economic losses because of vehicle crashes. Apart from crash data from real trials, NHTSA provides several simulation models [7, 8, 27] and finite element vehicle models as well. There are several types of collision tests that NHTSA conducts, but Authors focus on frontal collisions only [13].

2. Tensor product method description

Let us assume that there are given points $(x_n, y_n, z_n)_{n=1}^{N}$ and function family $(h_m)_{m=1}^{M}$ (functions of two variables). Again, the objective is to obtain the coefficients $(a_m)_{m=1}^{M}$, which minimize its value.

$$\sum_{n=1}^{N}\left(z_n - \sum_{m=1}^{M} a_m h(x_n, y_n)\right)^2 \tag{3}$$

Similarly to section 2, the issue of least square approximation is reduced to a linear solution:

$$\begin{pmatrix} \sum_{n=1}^{N} h_1(x_n, y_n) h_1(x_n, y_n) & \cdots & \sum_{n=1}^{N} h_1(x_n, y_n) h_M(x_n, y_n) \\ \vdots & \ddots & \vdots \\ \sum_{n=1}^{N} h_M(x_n, y_n) h_1(x_n, y_n) & \cdots & \sum_{n=1}^{N} h_M(x_n, y_n) h_M(x_n, y_n) \end{pmatrix} \begin{pmatrix} a_1 \\ \vdots \\ a_M \end{pmatrix} = \begin{pmatrix} \sum_{n=1}^{N} y_n h_1(x_n) \\ \vdots \\ \sum_{n=1}^{N} y_n h_M(x_n) \end{pmatrix} \tag{4}$$

https://doi.org/10.14669/AM.VOL95.ART4

As for the choice of function $(h_m)_{n=1}^{M}$, Legendre polynomial product tensors are chosen. Consideration involves a sequence of polynomials (P_m) defined by a iterative formula:

$$\forall_m \geq 1 (m+1)P_{m+1}(x) = (2m+1)x \cdot P_m(x) - nP_{m-1}(x) \quad (5)$$

Where $P_0(x)=1$ and $P_1(x)=x$. These are Legendre polynomials from a range of [–1,1]. First Legendre polynomials are:

$$P_0(x) = 1,\ P_1(x) = x, P_2(x) = \frac{1}{2}(3x^2 - 1), P_3(x) = \frac{1}{2}(5x^3 - 3x), \ldots \quad (6)$$

Legendre polynomials have a feature called orthogonality:

$$\forall_{i \neq j} \int_{-1}^{1} P_i(x) P_j(x)\, \mathrm{d}x = 0 \quad (7)$$

This feature is a natural consequence of Legendre polynomials being created as a result of orthogonalization of Gram–Schmidt function family $\{1, x, x^2, x^3, \ldots\}$. Orthogonality is valuable in this case, because the matrix M on left hand side (4) is closer to diagonal matrix. This results in smaller error of coefficients $(a_m)_{n=1}^{M}$.

In this application, Legendre polynomials sequence is renumbered so $Q_m=P_{m-1}$. Then following is obtained:

$$\forall_{m \geq 3} (m-1)Q_m(x) = (2m-3)x \cdot Q_{m-1}(x) - (m-2)Q_{m-2}(x) \quad (8)$$

where $Q_1(x)=1$ and $Q_2(x)=x$. To rescale the polynomials for arbitrary interval $[a,b]$, the following relation is used:

$$f_m(x) = Q_m\left(\frac{2x - a - b}{b - a}\right) \quad (9)$$

Finally, the tensor product of two function f, g is described as:

$$h(x, y) = f \otimes g(x, y) = f(x)g(y) \quad (10)$$

In this application the $(f_i)_{i=1}^{3}$. and $(g_j)_{j=1}^{3}$ are the first five Legendre polynomials. This gives 9 tensor products:

$$\begin{aligned} &h_1 = f_1 \otimes g_1, \quad h_2 = f_1 \otimes g_2, \quad h_3 = f_1 \otimes g_3, \\ &h_4 = f_2 \otimes g_1, \quad h_5 = f_2 \otimes g_2, \quad h_6 = f_2 \otimes g_3, \\ &h_7 = f_3 \otimes g_1, \quad h_8 = f_3 \otimes g_2, \quad h_9 = f_3 \otimes g_3. \end{aligned}$$

3. Results of tensor product method

The database consists of 260 crash tests. Model was created based on all cases and then validated. Authors prepared the algorithm that returns following factors:

$a_1 = 14.306917, a_2 = 2.295384, a_3 = -0.783896, a_4 = -0.561121, a_5 = 1.259176,$
$\mathrm{a}_6 = -1.059879, \mathrm{a}_7 = -0.627149, \mathrm{a}_8 = 1.396847, \mathrm{a}_9 = -0.872245$

https://doi.org/10.14669/AM.VOL95.ART4

Final equation takes the form below:

$$\begin{aligned} EES = & -0{,}21806125(11{,}86483271240814(2Cs - 0{,}95236)^2 \\ & - 1)(4{,}19031882290646810^{-8}(2m - 2360{,}1)^2 - 1) \\ & + 1{,}38895772014955(2Cs \\ & - 0{,}95236)(4{,}19031882290646810^{-8}(2m - 2360{,}1)^2 - 1) \\ & - 0{,}3135745(4{,}19031882290646810^{-8}(2m - 2360{,}1)^2 - 1) \\ & + 6{,}26309786912176810^{-5}(11{,}86483271240814(2Cs - 0{,}95236)^2 \\ & - 1)(2m - 2360{,}1) \\ & - 2{,}95950805412516510^{-4}(2Cs - 0{,}95236)(2m - 2360{,}1) \\ & + 6{,}63161689102147610^{-5}(2m - 2360{,}1) \\ & - 0{,}391948(11{,}86483271240814(2Cs - 0{,}95236)^2 - 1) \end{aligned} \tag{11}$$

The plot of Legendre polynomials tensor product approximation is presented in Figure 1.

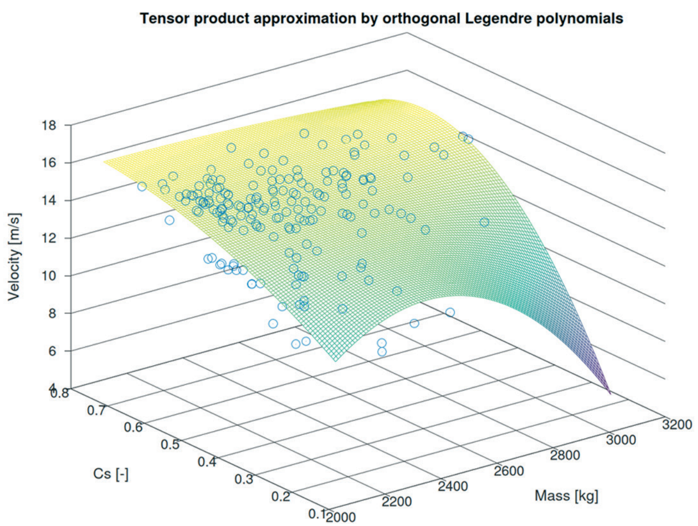

Fig. 1. Tensor product approximation by orthogonal Legendre polynomials, that clearly shows the advantage over linear model in terms of data fitting

And for the purpose of comparison, Figure 2 shows the linear approximation of analyzed data.

https://doi.org/10.14669/AM.VOL95.ART4

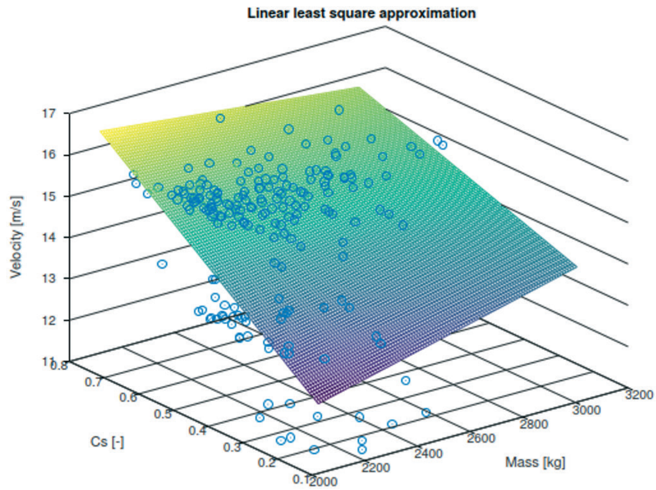

Fig. 2. Linear least square approximation

The average value of relative error for nonlinear method for Luxury class is 6.83% as presented in Figure 3. At the same time the error for linear method is equal to 6.99% as shown in Figure 4. The difference in this case is not significant and this is due to the size of the car itself. The ability to absorb deformations in case of modern and older cars is quite similar. In case of smaller cars, e.g. compact vehicle class, the difference between those approaches is better visible.

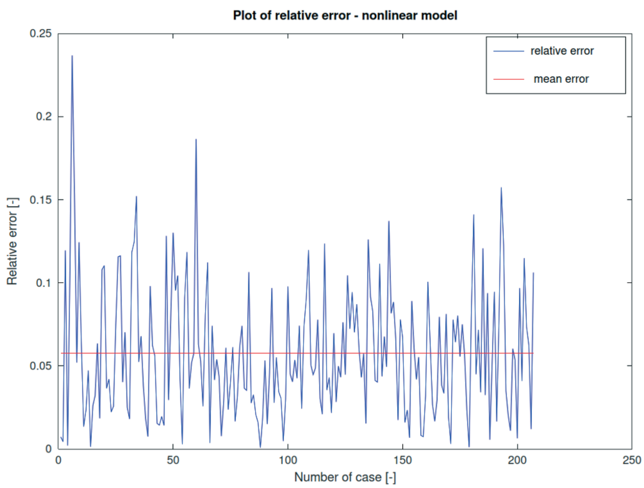

Fig. 3. Value of relative error in nonlinear model (6.83%)

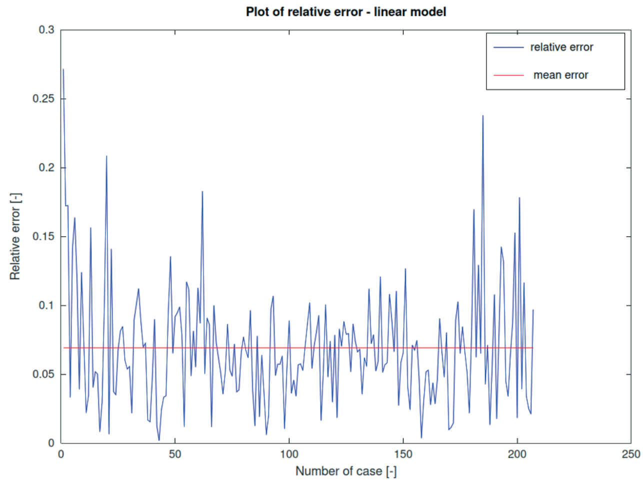

Fig. 4. Value of relative error in linear model (6.99%)

Figure 5 presents an overview of linear and nonlinear approach accuracy comparison. In this case it is clearly visible that the velocity determined using nonlinear method is in each closer to the real value, than the linear approach.

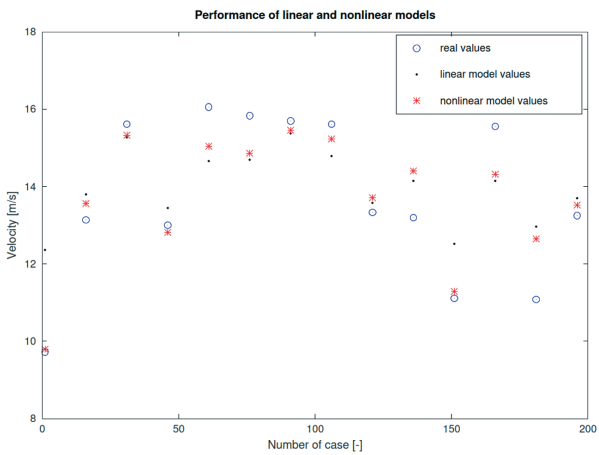

Fig. 5. Performance of linear and nonlinear models (Legendre tensor product)

Following Table 1 presents detailed data for Legendre approach in a group of selected cases.

https://doi.org/10.14669/AM.VOL95.ART4

Table 1. Detailed numerical values of the inverse method

m	C_s	V_t	Expected linear	Expected nonlinear	Linear error	Nonlinear error
2195	0.158300	15.722222	12.786543	12.577140	0.186722	0.200041
2270	0.532100	13.555556	15.082194	15.102688	0.112621	0.114133
2375	0.557400	13.416667	15.238359	15.221886	0.135778	0.134550
2145	0.501100	15.722222	14.865544	14.922967	0.054488	0.050836
2678	0.632900	15.722222	15.591482	15.596647	0.008316	0.007987
2139	0.578300	15.750000	15.350977	15.345375	0.025335	0.025690
2106	0.383600	13.500000	14.098811	14.059705	0.044356	0.041460
2092	0.401500	15.694444	14.204831	14.174748	0.094913	0.096830
2367	0.428400	13.333333	14.530677	14.656792	0.089801	0.099259
2123	0.496800	15.638889	14.831857	14.890327	0.051604	0.047865
2339	0.508300	15.750000	14.961309	15.007294	0.050076	0.047156
2631	0.465200	15.647222	14.842471	14.863949	0.051431	0.050058
2706	0.567200	15.647222	15.307008	15.394504	0.021743	0.016151
2111	0.443200	13.322222	14.484543	14.523834	0.087247	0.090196
2198	0.355800	15.736111	13.995030	14.068686	0.110642	0.105962
2368	0.242700	11.194444	13.514111	13.727558	0.207216	0.226283
2229	0.409900	15.722222	14.343968	14.452689	0.087663	0.080748
2224	0.359500	15.638889	14.038424	14.145599	0.102339	0.095486
2195	0.158300	15.722222	12.786543	12.577140	0.186722	0.200041

4. Calculation example

Exemplary calculations were made using the NHTSA crash test results. Table 2 includes test case data used to calculate the EES value. As mentioned in the Introduction, the deformation is being measured in six control points, as shown in Figure 6.

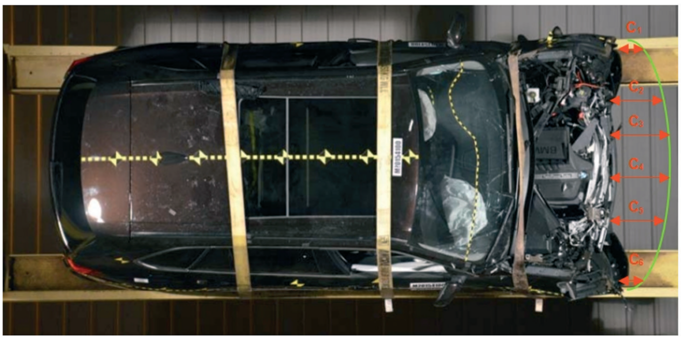

Fig. 6. Frontal deformation with method of measurements [41]

https://doi.org/10.14669/AM.VOL95.ART4

Table 2. Data used in calculations

Vehicle mass m	2112 kg
Crash velocity V_t	47.6 km/h=13.22 m/s
Elastic deformation velocity limit	11 km/h
Deformation width L_t	1.709 m
C_1	0.490 m
C_2	0.503 m
C_3	0.508 m
C_4	0.503 m
C_5	0.501 m
C_6	0.501 m

Coefficient C_s is calculated using formula (2) and is equal to 0.5021 [m].

Linear approach:

$$W_{def} = 256456 \text{ [J]}$$
$$EES = 15.58384 \left[\frac{m}{s}\right]$$
$$relative\ error = 17.861\%$$

Nonlinear approach:
Using values of vehicle mass m and coefficient C_s that are substituted into equation (11), the value of EES is calculated and yields following results:

$$EES = 12.53865 \left[\frac{\mathrm{m}}{\mathrm{s}}\right]$$
$$relative\ error = 5.154\%$$

5. Conclusions

Nonlinear method of vehicle velocity determination based on tensor product of Legendre polynomial shows promising results. Mean error for Luxury class is not much better than in linear ones, but the biggest advantage is visible in the figure 5. Velocity determined using nonlinear method is much more accurate than in linear ones. The difference is not as significant as in other vehicle classes described in papers published by the Authors, but the improvement is visible. Moreover, Authors are intending to develop this method further by adding more factors in order to lower the relative error even more.

Nevertheless, the improvement is clearly visible, especially when considering the whole spectrum of examined cases. Upon analyzing all the vehicle classes, authors intend to create a piece of software that will allow to apply this method in an easy and convenient way. The next step is to develop a handheld device that would estimate the precrash velocity upon 3D scanning the wrecked vehicle or using photogrammetry to find the deformation depth.

https://doi.org/10.14669/AM.VOL95.ART4

6. Nomenclature

EES	Equivalent Energy Speed [m/s]
NHTSA	National Highway Traffic Safety Administration
C_s	deformation ratio [m]
C_1–C_6	deformation coefficients
L_t	dent zone width [m]
V_t	vehicle speed [m/s]
W_{def}	work of deformation [J]
b_k	constant slope factor [m/s/m]
m	weight of car [kg]
n	number of cases [–]

References

[1] Axler S.J.: Linear Algebra Done Right; 2nd ed.; Springer: New York, NY, 1997; ISBN 9780387225951.

[2] Campbell B.J.: The Traffic Accident Data Project Scale. Proceedings of Collision Investigation Methodology Symposium. 1969, 675–681.

[3] Cao Y., Luo Y.F.: The Synthesized Method Based on Classical Mechanics and Finite Element for Vehicle Collision Accident Reconstruction Analysis. International Journal of Crashworthiness. 2021, 1–8, DOI: 10.1080/13588265.2021.2008741.

[4] Cheney W., Kincaid D.: Numerical Analysis: Mathematics of Scientific Computing. American Mathematical Society. Pure and Applied Undergraduate Texts. 2002, 2.

[5] Faraj R., Holnicki-Szulc J., Knap L., Seńko J.: Adaptive Inertial Shock-Absorber. Smart Materials and Structures. 2016, 25(3), DOI: 10.1088/0964-1726/25/3/035031.

[6] Geigl B.C., Hoschopf H., Steffan H., Moser A.: Reconstruction of Occupant Kinematics and Kinetics for Real World Accidents. International Journal of Crashworthiness. 2003, 8(1), 17–27, DOI: 10.1533/ijcr.2003.0217.

[7] Gidlewski M., Żardecki D.: Simulation-Based Sensitivity Studies of a Vehicle Motion Model. Proceedings of the 20th International Scientific Conference Transport Means 2016. 2016, 236–240.

[8] Grolleau V., Galpin B., Penin A., Rio G.: Modelling the Effect of Forming History in Impact Simulations: Evaluation of the Effect of Thickness Change and Strain Hardening Based on Experiments. International Journal of Crashworthiness. 2008, 13(4), 363–373, DOI: 10.1080/13588260801976120.

[9] Han I., Kang H., Park J.C., Ha Y.: Three-Dimensional Crush Measurement Methodologies Using Two-Dimensional Data. Transactions of the Korean Society of Automotive Engineers. 2015, 23(3), 254–262, DOI: 10.7467/ksae.2015.23.3.254.

[10] Han I.: Vehicle Collision Analysis from Estimated Crush Volume for Accident Reconstruction. International Journal of Crashworthiness. 2019, 24(1), 100–105, DOI: 10.1080/13588265.2018.1440499.

[11] Han I.: Analysis of Vehicle Collision Accidents Based on Qualitative Mechanics. Forensic Science International. 2018, 291, 53–61, DOI:10.1016/j.forsciint.2018.08.004.

[12] Hight P.V., Fugger T.F., Marcosky J.: Automobile Damage Scales and the Effect on Injury Analysis. SAE Technical Paper. 1992, 920602, DOI: 10.4271/920602.

[13] Iraeus J., Lindquist M.: Pulse Shape Analysis and Data Reduction of Real-Life Frontal Crashes with Modern Passenger Cars. International Journal of Crashworthiness. 2015, 20(6), 535–546, DOI: 10.1080/13588265.2015.1057005.

[14] Krukowski M., Kubiak P., Mrowicki A., Siczek K., Gralewski J.: Non-Linear Method of Determining Vehicle Pre-Crash Speed Based on Tensor B-Spline Products with Probabilistic Weights – Intermediate Car Class. Forensic Science International. 2018, 293, 7–16, DOI: 10.1016/j.forsciint.2018.10.011.

[15] Kubiak P.: Work of Non-Elastic Deformation against the Deformation Ratio of the Subcompact Car Class Using the Variable Correlation Method. Forensic Science International. 2018, 287, 47–53, DOI: 10.1016/j.forsciint.2018.03.033.

[16] Lindquist M., Hall A., Björnstig U.: Real World Car Crash Investigations – A New Approach. International Journal of Crashworthiness. 2003, 8(4), 375–384, DOI:10.1533/ijcr.2003.0245.

[17] Mackay G.M., Hill J., Parkin S., Munns J.A.: Restrained Occupants on the Nonstruck Side in Lateral Collisions. Accident Analysis & Prevention. 1993, 25(2), 147–152, DOI: 10.1016/0001-4575(93)90054-z.

[18] Mannering F., Bhat C.R.: Analytic Methods in Accident Research: Methodological Frontier and Future Directions. Analytic Methods in Accident Research. 2014, 1, 1–22, DOI: 10.1016/j.amar.2013.09.001.

[19] Mchenry B.G.: The Algorithms of CRASH. Southeast Coast Collision Conference. 2001, Cocoa Beach, Florida.

[20] Mchenry R.R.: Computer Program for Reconstruction of Highway Accidents. SAE Technical Paper.1973, DOI: 10.4271/730980.

[21] Nelson W.D.: The History and Evolution of the Collision Deformation Classification SAE J224 MAR80. SAE Technical Paper. 1981, 90232, DOI: 10.4271/810213.

[22] Norros I., Kuusela P., Innamaa S., Pilli-Sihvola E., Rajamäki R.: The Palm Distribution of Traffic Conditions and Its Application to Accident Risk Assessment. Analytic Methods in Accident Research. 2016, 12, 48–65, DOI: 10.1016/j.amar.2016.10.002.

[23] Prochowski L., Ziubinski M., Gidlewski M.: Experimental and Analytic Determining of Changes in Motor Cars' Positions in Relation to Each Other during a Crash Test Carried out to the FMVSS 214 Procedure. XI International Science-Technical Conference Automotive Safety. 2018, 136991, 1–5, DOI: 10.1109/AUTOSAFE.2018.8373302.

[24] Prochowski L., Gidlewski M., Ziubiński M., Dziewiecki K.: Kinematics of the Motorcar Body Side Deformation Process during Front-to-Side Vehicle Collision and the Emergence of a Hazard to Car Occupants. Meccanica. 2021, 56(4), 901–922, DOI: 10.1007/s11012-020-01274-3.

[25] Neptune J.A.: Crush Stiffness Coefficients, Restitution Constants, and a Revision of CRASH3 & SMAC. SAE Technical Paper. 1998, 90116, DOI: 10.4271/980029.

[26] Ptak M., Wilhelm J., Klimas O., Reclik G., Garbaciak L.: Numerical Simulation of a Motorcycle to Road Barrier Impact. Lecture Notes in Mechanical Engineering. 2019, 565–573, DOI: 10.1007/978-3-030-04975-1_65.

[27] Sharma D., Stern S., Brophy J., Choi E.: An Overview of NHTSA's Crash Reconstruction Software WinSMASH. Proceedings of the 20th International Technical Conference on Enhanced Safety of Vehicles. 2007, Lyon, France.

[28] Siddall D.E., Day T.D.: Updating the Vehicle Class Categories. SAE Technical Paper. 1996, 90323, DOI: 10.4271/960897.

[29] Syad B.A., Salmani E., Ez-Zahraouy H., Benyoussef A.: Computational Method of the Stiffness Coefficients A and B in the Case of Frontal Impact from the Results of the Crash Tests. International Journal of Intelligent Transportation Systems Research. 2021, 19(3), 587–593, DOI: 10.1007/s13177-021-00266-1.

[30] Vangi D., Cialdai C.: Evaluation of Energy Loss in Motorcycle-to-Car Collisions. International Journal of Crashworthiness. 2014, 19(4), 361–370, DOI: 10.1080/13588265.2014.899072.

[31] Vangi D.: Simplified Method for Evaluating Energy Loss in Vehicle Collisions. Accident Analysis & Prevention. 2009, 41(3), 633–641, DOI: 10.1016/j.aap.2009.02.012.

[32] Vangi D.: Vehicle Collision Dynamics: Analysis and Reconstruction. Butterworth-Heinemann, 2020.

https://doi.org/10.14669/AM.VOL95.ART4

[33] Vangi D., Cialdai C., Gulino M.S.: Vehicle Stiffness Assessment for Energy Loss Evaluation in Vehicle Impacts. Forensic Science International. 2019, 300, 136–144, DOI: 10.1016/j.forsciint.2019.04.031.

[34] Vangi D., Begani F., Spitzhüttl F., Gulino M.S.: Vehicle Accident Reconstruction by a Reduced Order Impact Model. Forensic Science International. 2019, 298, 426.e1–426.e11, DOI: 10.1016/j.forsciint.2019.02.042.

[35] Wach W.: Reconstruction of Vehicle Kinematics by Transformations of Raw Measurement Data. XI International Science-Technical Conference Automotive Safety 2018. 2018, 136991, 1–5, DOI: 10.1109/AUTOSAFE.2018.8373324.

[36] Wach W.: Spatial Impulse-Momentum Collision Model in Programs for Simulation of Vehicle Accidents. XII International Science-Technical Conference Automotive Safety 2020. 2020, 9293494, DOI: 10.1109/AUTOMOTIVESAFETY47494.2020.9293494.

[37] Wood D.P., Simms C.K.: Car Size and Injury Risk: A Model for Injury Risk in Frontal Collisions. Accident Analysis & Prevention. 2002, 34(1), 93–99, DOI: 10.1016/s0001-4575(01)00003-3.

[38] Żuchowski A.: The Use of Energy Methods at the Calculation of Vehicle Impact Velocity. The Archives of Automotive Engineering – Archiwum Motoryzacji. 2015, 68(2), 85–111.